

RESEARCH ARTICLE | SEPTEMBER 10 2012

Refined theoretical study of radiative association: Cross sections and rate constants for the formation of SiN

Magnus Gustafsson; Sergey V. Antipov; Jan Franz; Gunnar Nyman



J. Chem. Phys. 137, 104301 (2012)

<https://doi.org/10.1063/1.4750029>



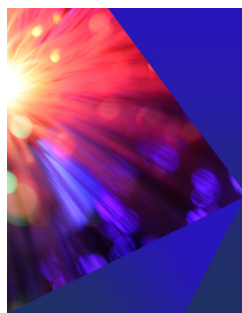
View
Online



Export
Citation

CrossMark

This article may be downloaded for personal use only. Any other use requires prior permission of the author and AIP Publishing. This article appeared in (citation of published article) and may be found at <https://doi.org/10.1063/1.4750029>



The Journal of Chemical Physics
2024 Emerging Investigators
Special Collection

Submit Today

Refined theoretical study of radiative association: Cross sections and rate constants for the formation of SiN

Magnus Gustafsson,^{a)} Sergey V. Antipov, Jan Franz,^{b)} and Gunnar Nyman
Department of Chemistry and Molecular Biology, University of Gothenburg, 41296 Gothenburg, Sweden

(Received 20 April 2012; accepted 21 August 2012; published online 10 September 2012)

Radiative association of silicon mononitride (SiN) in its two lowest molecular electronic states is studied through quantum and classical dynamics. Special attention is paid to the behavior of the cross section at high collision energies. A modified expression for the semiclassical cross section is presented which excludes transitions to continuum states. This gives improved agreement with quantum mechanical perturbation theory at high energies. The high energy cross section is overestimated if conventional semiclassical theory is used. The modified semiclassical theory should be valid in general for radiative association transitions from an upper to a lower electronic state. We also implement a quantum dynamical optical potential method with the same type of modification. The rate coefficient is calculated using Breit–Wigner theory and the modified semiclassical formula for the resonance and direct contributions, respectively, for temperatures from 10 K to 20 000 K. A rapid decrease in the rate constant for formation of ground state SiN is observed above 2000 K which was not seen previously. © 2012 American Institute of Physics. [<http://dx.doi.org/10.1063/1.4750029>]

I. INTRODUCTION

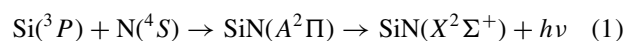
Understanding molecular formation is of central interest in chemistry. To form a diatomic molecule from two free atoms requires that energy is removed so that a bound state of the molecule can be reached. Under normal conditions on Earth this typically happens by a third body carrying away the energy. If the density is extremely low, however, three body collisions become very unlikely and radiative association can be important. In radiative association a photon is emitted to stabilize the molecule. In forming a diatom this emission has to be fast as the atoms are only close for a short period of time since the translational energy cannot be redistributed into vibrational motion.

In this paper we review and compare some ways of calculating cross sections for radiative association of diatomic molecules. The methods include perturbation theory,¹ a quantum dynamical optical potential (OP) approach,^{2,3} a semiclassical implementation⁴ and Breit–Wigner (BW) theory.^{5,6}

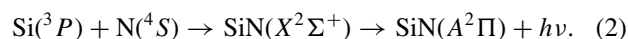
Quantum mechanical perturbation theory is popular for treating radiative association. The resulting cross section generally displays striking resonance features superimposed on a smooth baseline. The resonances stem from quasibound states that are supported by a barrier in the effective potential, and the baseline is produced by direct (nonresonant) radiative association. While perturbation theory works well, it overestimates the cross section for resonances where the tunneling width is comparable to or smaller than the lifetime broadening of the radiative decay.^{7,8} For those resonances quantum dynamics with an explicit optical potential offers an alternative which is also quite convenient computationally. It has, however, other limitations which we will return to below.

The semiclassical method is based on classical trajectories and does therefore not contain the resonance structure in the cross sections. The resonances can be important to include in order to obtain the thermal rate constant accurately at low temperature. Breit–Wigner theory only describes the resonances and not the direct contribution. Thus, combining the semiclassical approach with the Breit–Wigner method can be a useful strategy. In this work one aim is to understand how well this works by comparing the various methods. These comparisons lead us to propose a modification of the theory, which affects both the optical potential and the semiclassical implementations. We apply the discussed methods to the formation of silicon mononitride (SiN).

The silicon atom has a ³P ground electronic state and the nitrogen atom a ⁴S state. As the atoms approach, the nine spin-orbit states of Si(³P) can be combined with the four spin-orbit states of N(⁴S) to form 36 molecular spin-orbit states. These states can be of doublet, quartet, and sextet multiplicities but here we restrict ourselves to study radiative association involving only the two lowest doublet states, viz.,



and



Spin-orbit and rotational couplings should in general be taken into account in radiative association. Their effect has been investigated in the formation of the cyano radical (CN) where, for example, their role in the low energy cross section was demonstrated.⁹ In this work spin-orbit and rotational couplings are excluded. Note that for atom–atom collisions, in the absence of those couplings, only shape resonances (no Feshbach resonances) are possible.

Reaction (1) has been studied semiclassically by Singh *et al.*¹⁰ We use the same *ab initio* data as Singh *et al.* for

^{a)}Electronic mail: magnu@chem.gu.se.

^{b)}Present address: Mulliken Center for Theoretical Chemistry, University of Bonn, Beringstr. 4-6, 53115 Bonn, Germany.

the potential energy curves and transition dipole moments, which they calculated at multireference configuration interaction (MRCI) level with correlated consistent polarized valence quadrupole zeta (cc-pVQZ)^{11,12} basis functions.

We note that SiN has been detected in the circumstellar envelope of the carbon rich star IRC+10216¹³ and in the interstellar medium.¹⁴ The SiN formation rate is thus of importance in astrochemistry and we calculate the rate constant over the temperature interval 10 K–20 000 K.

II. THEORY

The rate constant at a given temperature T for formation of SiN by radiative association according to reaction (1) or (2) can be written as

$$k_{\Lambda \rightarrow \Lambda'}(T) = \left(\frac{8}{\mu\pi}\right)^{1/2} \left(\frac{1}{k_B T}\right)^{3/2} \int_0^\infty E \sigma_{\Lambda \rightarrow \Lambda'}(E) e^{-E/k_B T} dE, \quad (3)$$

where μ is the reduced mass, k_B is the Boltzmann constant, and E is the collisional energy. Λ and Λ' indicate the orbital electronic angular momentum, projected on the molecular axis, of the initial state (of approach) and the final (bound) state, respectively. Since only doublet states of the diatomic system are considered we frequently refer to reactions (1) and (2) as $\Pi \rightarrow \Sigma$ and $\Sigma \rightarrow \Pi$, respectively, without indicating the spin multiplicity or the reflection symmetry.

The cross section $\sigma_{\Lambda \rightarrow \Lambda'}$ can be computed by a number of different approaches. In this section we will outline four of those, each with its merit in the study of radiative association.

A. Perturbation theory

We will begin with a brief summary of the established quantum mechanical perturbation theory for radiative association. The Fermi golden rule cross section for the process can be expressed as^{1,15}

$$\sigma_{\Lambda \rightarrow \Lambda'}(E) = \frac{64}{3} \frac{\pi^5 \hbar^2}{(4\pi\epsilon_0)c^3} \frac{1}{2\mu E} P_\Lambda \times \sum_{v'J'J} v_{E\Lambda'\nu'J'}^3 S_{\Lambda J \rightarrow \Lambda' J'} M_{\Lambda E J, \Lambda' \nu' J'}^2, \quad (4)$$

where the sum is over all initial rotational (J) and final vibrational (v') and rotational (J') quantum numbers. The speed of light is c , the frequency of the emitted photon is $\nu_{E\Lambda'\nu'J'}$, and $S_{\Lambda J \rightarrow \Lambda' J'}$ are the Hönl–London factors given in Table I. The statistical weight factor for approaching in the initial molecular electronic state Λ is given by (see, e.g., Andreatza, Singh, and Sanzovo¹⁶)

$$P_\Lambda = \frac{(2S+1)(2-\delta_{0,\Lambda})}{(2L_{\text{Si}}+1)(2S_{\text{Si}}+1)(2L_{\text{N}}+1)(2S_{\text{N}}+1)}, \quad (5)$$

where $L_{\text{Si}} = 1$, $S_{\text{Si}} = 1$, $L_{\text{N}} = 0$, $S_{\text{N}} = 3/2$, are the electronic orbital angular momentum and spin quantum numbers of the atoms and $\Lambda = 0$ or 1 for the Σ or Π molecular states, respectively. We consider only doublet states of SiN, so that the total electronic spin is $S = 1/2$. The values of P_Λ are given in Table II.

TABLE I. Hönl–London factors, $S_{\Lambda J \rightarrow \Lambda' J'}$ of Watson.¹⁷ See also the discussion in the Appendix.

J'	$A^2\Pi \rightarrow X^2\Sigma^+$	$X^2\Sigma^+ \rightarrow A^2\Pi$
$J-1$	$(J+1)/2$	$J-1$
J	$(2J+1)/2$	$2J+1$
$J+1$	$J/2$	$J+2$

The transition dipole matrix element is given by the integral

$$M_{\Lambda E J, \Lambda' \nu' J'} = \int_0^\infty F_{EJ}^\Lambda(R) D(R) \Phi_{\nu' J'}^{\Lambda'}(R) dr, \quad (6)$$

where $D(R)$ is the matrix element of the dipole moment operator between the two molecular electronic states ($X^2\Sigma^+$ and $A^2\Pi$) as a function of the internuclear distance R . $F_{EJ}^\Lambda(R)$ is the continuum wave function of the initial state for the partial wave J , normalized to the collision energy E (see, e.g., Landau and Lifshitz¹⁸) and $\Phi_{\nu' J'}^{\Lambda'}(R)$ is a bound state wave function, normalized to unity. In Eqs. (4) and (6) above we have applied the approximation for the total angular momentum and spin that $\mathbf{J} - \mathbf{S} \approx \mathbf{J}$ (see, e.g., Babb and Dalgarno¹).

B. Optical potential method

The explicit optical potential method can be efficient since it does not necessarily require the calculation of bound states. It has been applied before to radiative charge transfer³ and radiative quenching.¹⁹ The optical potential for the system under consideration reads

$$V_{\text{opt}}(R) = -\frac{i\hbar}{2} A_{\Lambda \rightarrow \Lambda'}(R), \quad (7)$$

where

$$A_{\Lambda \rightarrow \Lambda'}(R) = \frac{64}{3} \frac{\pi^4}{(4\pi\epsilon_0)hc^3} \left(\frac{2-\delta_{0,\Lambda+\Lambda'}}{2-\delta_{0,\Lambda}}\right) \nu_{\Lambda \rightarrow \Lambda'}^3(R) D^2(R) \quad (8)$$

is the transition probability (with dimension time⁻¹) and

$$\nu_{\Lambda \rightarrow \Lambda'}(R) = \frac{\max(0, V_\Lambda(R) - V_{\Lambda'}(R))}{h} \quad (9)$$

is the photon frequency which, including the max function, follows from the stationary phase approximation,²⁰ or equivalently, the classical Franck–Condon principle; the relative momentum and positions of the atoms are conserved during radiative transitions. The form of Eq. (9) is convenient in our study of SiN where it applies to both transitions $\Pi \rightarrow \Sigma$ (for $R < 3.28$ bohrs, see Fig. 1) and $\Sigma \rightarrow \Pi$ (for $R > 3.28$ bohrs). Note that calculations based on Eqs. (7)–(9) are limited to

TABLE II. Statistical weights.

	$A^2\Pi \rightarrow X^2\Sigma^+$	$X^2\Sigma^+ \rightarrow A^2\Pi$
P_Λ	4/36	2/36
$\frac{2-\delta_{0,\Lambda+\Lambda'}}{2-\delta_{0,\Lambda}}$	1	2

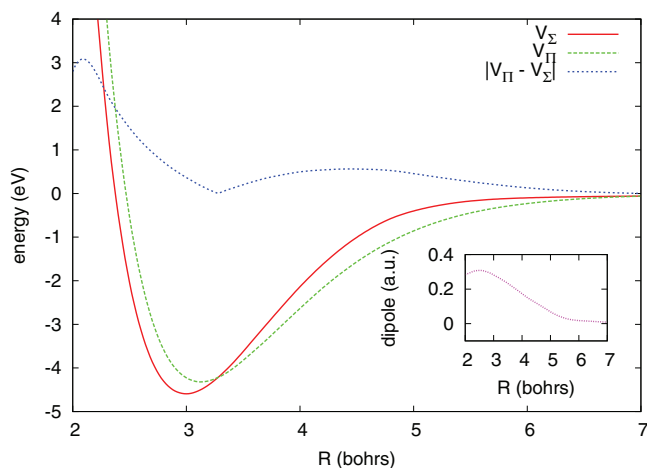


FIG. 1. Potential energy curves for SiN in the $X^2\Sigma^+$ state (red) and $A^2\Pi$ state (green). Also shown is the magnitude of the difference between them (blue), and the $X^2\Sigma^+ \leftrightarrow A^2\Pi$ transition dipole moment $D(R)$ (pink). The data is taken from Singh *et al.*¹⁰

transitions from an upper to a lower electronic state. This theory can thus not be applied to, e.g., $X^2\Sigma^+ \rightarrow X^2\Sigma^+$ transitions. This is also a limitation of the semiclassical theory which is outlined in Sec. II C.

The completeness of the final states was applied in the derivation of Eqs. (7)–(9). This means that spontaneous emission to both bound and continuum final states is included.¹⁵ The emission corresponds to molecule formation through radiative association only when the final state is bound. In order to obtain the cross section for this process we define a restricted transition probability

$$A_{\Lambda \rightarrow \Lambda'}^{EJ}(R) = \begin{cases} A_{\Lambda \rightarrow \Lambda'}(R) & \text{if } E < V_{\Lambda}(R) - V_{\Lambda'}(R) \text{ and} \\ & V_{\Lambda'}(R) + \frac{\hbar^2 J(J+1)}{2\mu R^2} < 0 \\ 0 & \text{otherwise} \end{cases}, \quad (10)$$

where the first condition ensures transitions to bound states, and the second condition checks that bound states are supported (excluding the zero point energy) on the final effective potential. The angular momentum term in the final effective potential is approximate ($J' \approx J$ and $\Lambda' \approx 0$) but the formula mainly comes into play for large J and then it is a good approximation.

The Schrödinger equation with the optical potential reads

$$\left\{ -\frac{\hbar^2}{2\mu} \frac{d^2}{dR^2} + \frac{\hbar^2(J(J+1) - \Lambda^2)}{2\mu R^2} + V_{\Lambda}(R) - \frac{i\hbar}{2} A_{\Lambda \rightarrow \Lambda'}^{EJ}(R) - E \right\} F_{EJ}^{\Lambda \rightarrow \Lambda'}(R) = 0 \quad (11)$$

and the cross section for radiative association is given by

$$\sigma_{\Lambda \rightarrow \Lambda'}(E) = \frac{\pi \hbar^2}{2\mu E} P_{\Lambda} \sum_J (2J+1) (1 - e^{-4\eta_{EJ}^{\Lambda \rightarrow \Lambda'}}), \quad (12)$$

where $\eta_{EJ}^{\Lambda \rightarrow \Lambda'}$ is the imaginary part of the phase shift of $F_{EJ}^{\Lambda \rightarrow \Lambda'}(R)$. A real phase shift gives a unitary S -matrix and the cross section (12) is thus determined by the loss of unitarity.

C. Semiclassical limit

From their optical potential formalism Zygelman and Dalgarno¹⁹ rederived the semiclassical cross section originally put forward by Bates.⁴ They did this by application of the distorted wave and JWKB approximations, and by changing the partial wave (J) summation to an impact parameter integration. In the same way we obtain from Eq. (12) the cross section

$$\sigma_{\Lambda \rightarrow \Lambda'}(E) = 4\pi \left(\frac{\mu}{2E} \right)^{1/2} P_{\Lambda} \int_0^{\infty} b \times \int_{R_c}^{\infty} \frac{A_{\Lambda \rightarrow \Lambda'}^{Eb}(R) dR db}{(1 - V_{\Lambda}(R)/E - b^2/R^2)^{1/2}}, \quad (13)$$

where b is the impact parameter, for which R_c is the outer classical turning point on the potential V_{Λ} . The restricted transition probability

$$A_{\Lambda \rightarrow \Lambda'}^{Eb}(R) = \begin{cases} A_{\Lambda \rightarrow \Lambda'}(R) & \text{if } E < V_{\Lambda}(R) - V_{\Lambda'}(R) \text{ and} \\ & V_{\Lambda'}(R) + \frac{Eb^2}{R^2} < 0 \\ 0 & \text{otherwise} \end{cases} \quad (14)$$

is defined similarly to that in Sec. II B, now with the classical expression for the centrifugal energy in the final effective potential.

D. Breit–Wigner theory

In Sec. II B we have presented a quantum mechanical theory which should correctly predict the cross section, even for resonances corresponding to very long-lived quasibound states.² The total width of these peaks is, however, so small that a straightforward integration of the cross section to obtain the rate constant is not feasible. The established method to compute the resonance contribution to the rate for radiative association is the Breit–Wigner theory.^{5,6} The cross section due to resonances with rotation J and vibration v is

$$\sigma_{\Lambda \rightarrow \Lambda'}(E) = \frac{\pi \hbar^2}{2\mu E} P_{\Lambda} \sum_{vJ} (2J+1) \times \frac{\Gamma_{vJ\Lambda \rightarrow \Lambda'}^{\text{rad}} \Gamma_{vJ\Lambda}^{\text{tun}}}{(E - E_{vJ\Lambda})^2 + (\Gamma_{vJ\Lambda}^{\text{tun}} + \Gamma_{vJ\Lambda \rightarrow \Lambda'}^{\text{rad}})^2 / 4}, \quad (15)$$

where the radiative width, $\Gamma_{vJ\Lambda \rightarrow \Lambda'}^{\text{rad}}$ (summed over all final rovibrational states), the tunneling width, $\Gamma_{vJ\Lambda}^{\text{tun}}$, and the resonance energies $E_{vJ\Lambda}$ can be computed efficiently, e.g., by application of the Airy boundary condition in the scattering calculation.^{21,22} The resonance component of the rate coefficient

$$k_{\Lambda \rightarrow \Lambda'}(T) = \hbar^2 P_{\Lambda} \left(\frac{2\pi}{\mu k_B T} \right)^{3/2} \sum_{vJ} (2J+1) \times \frac{e^{-E_{vJ\Lambda}/k_B T}}{1/\Gamma_{vJ\Lambda}^{\text{tun}} + 1/\Gamma_{vJ\Lambda \rightarrow \Lambda'}^{\text{rad}}} \quad (16)$$

is obtained by integration of Eq. (3) with the cross section (15) inserted and assuming that the widths of the resonances are small compared to the thermal energy.

III. COMPUTATIONAL DETAILS

For the potential energy curves and transition dipole moment function the data of Ref. 10 are used (see Fig. 1). The wave functions $\Phi_{v'J'}^{\Lambda'}(R)$ of the final bound states in Eq. (6) are obtained by solving the Schrödinger equation with the discrete variable representation method of Colbert and Miller.²³ The time-independent wave functions $F_{EJ}(R)$ of the continuum states in Eqs. (6) and (11) are computed with the Numerov method.²⁴ Numerical integration of the semiclassical cross section (13) is very fast and no elaborate method is necessary. In the R -dimension we have, however, applied a Romberg integration (original implementation in Ref. 25) to manage the integrand's behaviour as $R \rightarrow R_c^+$.

The resonance parameters in Eqs. (15) and (16) have been computed using LEVEL.²² With regards to the radiative widths $\Gamma_{vJ\Lambda \rightarrow \Lambda'}^{\text{rad}}$ it should be noted that LEVEL has Hönl–London factors implemented for singlet molecular states by default. Fortunately, for $\Sigma \rightarrow \Pi$ transitions, these agree with the values for doublets in Table I. For $\Pi \rightarrow \Sigma$ some care, however, has to be applied. LEVEL provides contributions corresponding to lines 3 and 4 in Table IV. Adding these and dividing by two gives a radiative width which is averaged over the initial parity, and $\Gamma_{vJ\Lambda \rightarrow \Lambda'}^{\text{rad}}$ is then effectively calculated using the Hönl–London factors of Table I.

IV. RESULTS

Figure 2 shows the cross sections computed using quantum mechanical perturbation theory and the semiclassical formula. The semiclassical calculation reproduces the quantum mechanical baseline for both transitions up to certain threshold energies of 1.95 eV and 0.563 eV for the $\Pi \rightarrow \Sigma$ and $\Sigma \rightarrow \Pi$ transitions, respectively. These energies can be in-

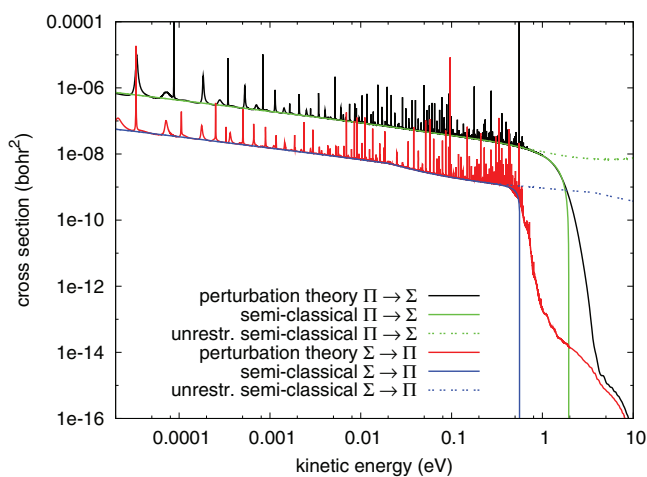


FIG. 2. Cross sections for forming SiN through radiative association, computed using quantum mechanical perturbation theory (Eq. (4)) and semiclassical theory (Eq. (13)). The semiclassical results obtained with an unrestricted transition probability according to Eq. (8) are also displayed.

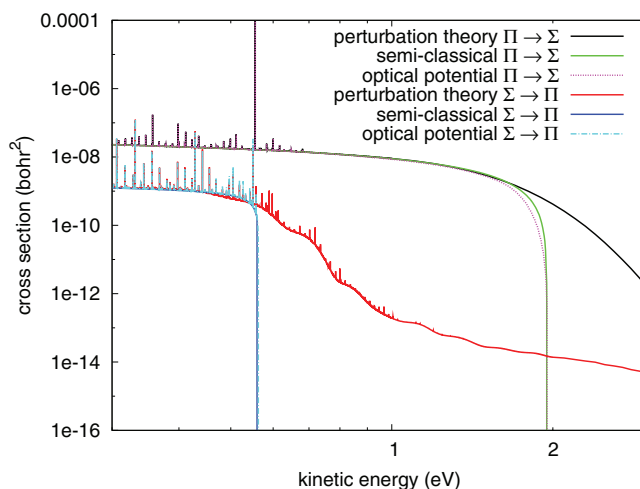


FIG. 3. Cross sections for forming SiN through radiative association around the threshold energies. Besides the results from perturbation theory (Eq. (4)) and semiclassical theory (Eq. (13)) we also display the quantum dynamical result using the optical potential method (Eq. (12)).

ferred from $|V_{\Pi} - V_{\Sigma}|$, which is displayed in Fig. 1. Above the threshold energies Franck–Condon transitions go to continuum rather than bound states and thus they do not represent molecule formation. To illustrate that mechanism we show in Fig. 2 the semiclassical results with the unrestricted transition probability $A_{\Lambda \rightarrow \Lambda'}(R)$ from Eq. (8) replacing $A_{\Lambda \rightarrow \Lambda'}^{Eb}(R)$ in Eq. (13). It is clear that the restriction on the transition probability in Eq. (14) is necessary to qualitatively reproduce the drop in the cross section above the threshold energy. The quantum cross section decreases fast above the threshold energy, but does not go to zero since it allows for molecule formation through non-Franck–Condon transitions.

In Fig. 3 the behaviour of the cross sections around the threshold energies is displayed. Here the cross section computed with the optical potential method is also shown. The baseline of that calculation is almost exactly reproduced by the semiclassical theory. The small discrepancy close to 2 eV for $\Pi \rightarrow \Sigma$ can be attributed to the difference in treatment close to the classical turning point. The wave function in Eq. (11) can penetrate the repulsive potential while the WKB wave function used in the derivation of Eq. (13) cannot. In fact the bound state condition on the transition probabilities in Eqs. (10) and (14) assumes no penetration of the potential so the semiclassical treatment is more consistent in this respect.

In Fig. 3 the resonance structure appears to be identical in the OP and perturbation treatments, except for at energies larger than the threshold for $\Sigma \rightarrow \Pi$ transitions where the OP cross section drops to zero. Many of the peaks are, however, extremely narrow and when they are resolved there is difference in height when the two approaches are compared. The optical potential method shows reasonable agreement (within about 8%) with BW theory for all five resonances shown in Table III. This is consistent with the conclusion that the resonances are correctly described with an optical potential,² from which the Breit–Wigner formula can be obtained.⁸ The modification in Eq. (10) does not appear to have any significant effect on the OP peak heights. For quasibound states with

TABLE III. Comparison of heights of five selected cross section peaks, four corresponding to quasibound states with tunneling width comparable with the radiative width and one (the last) with a much larger tunneling width. The columns labeled perturbation theory (PT), optical potential (OP), and Breit–Wigner (BW) show the peak heights in bohr² obtained with Eqs. (4), (12), and (15), respectively. The optical potential peak heights are determined both with and without the restriction in Eq. (10), OP and unr. OP, respectively. The resonance parameters used for BW (three last columns) are given in Hartree.

Transition	ν	J	PT	OP	Unr. OP	BW	$E_{\nu J \Lambda}$	$\Gamma_{\nu J \Lambda}^{\text{tun}}$	$\Gamma_{\nu J \Lambda \rightarrow \Lambda'}^{\text{rad}}$
$\Pi \rightarrow \Sigma$	53	61	1.3×10^2	0.40	0.40	0.419	6.607×10^{-4}	5.411×10^{-15}	8.740×10^{-14}
$\Pi \rightarrow \Sigma$	54	55	96	0.80	0.80	0.859	4.732×10^{-4}	7.920×10^{-15}	7.204×10^{-14}
$\Sigma \rightarrow \Pi$	46	65	36	0.70	0.73	0.691	4.492×10^{-4}	2.535×10^{-16}	1.649×10^{-15}
$\Sigma \rightarrow \Pi$	47	63	86	0.44	0.43	0.450	3.934×10^{-4}	1.615×10^{-16}	2.114×10^{-15}
$\Sigma \rightarrow \Pi$	47	65	6.3×10^{-5}	6.4×10^{-5}	6.4×10^{-5}	6.90×10^{-5}	5.285×10^{-4}	1.197×10^{-10}	1.624×10^{-15}

tunneling widths comparable with or smaller than their radiative widths (i.e., long-lived quasibound states) perturbation theory seriously overestimates the height of the peaks. This is a consequence of that the method has no built-in unitarity limit, or, in other words, it does not account for radiative broadening.⁷ Assuming that the resonance profiles computed with perturbation theory are perfectly Lorentzian, they are given by the BW cross section, Eq. (15), with $\Gamma_{\nu J \Lambda}^{\text{tun}}$ replacing $\Gamma_{\nu J \Lambda}^{\text{tun}} + \Gamma_{\nu J \Lambda \rightarrow \Lambda'}^{\text{rad}}$ in the denominator, and thus the peaks are too high by a factor $(1 + \Gamma_{\nu J \Lambda \rightarrow \Lambda'}^{\text{rad}} / \Gamma_{\nu J \Lambda}^{\text{tun}})^2$.

The direct component of the rate coefficient is displayed in Fig. 4. For each of the two transitions it is computed with Eq. (3) using cross sections obtained in three different ways:

1. *direct*: a combination of perturbation theory and semiclassical results. For $\Pi \rightarrow \Sigma$ transitions the semiclassical cross section is taken up to 0.7 eV and that of perturbation theory otherwise. For $\Sigma \rightarrow \Pi$ we take the semiclassical cross section up to 0.27 eV and selected points along the baseline of the perturbation theory cross section above that energy.
2. *semiclassical*: i.e., theory with the transition probability of Eq. (14).
3. *unrestricted semiclassical*: i.e., theory with the transition probability $A_{\Lambda \rightarrow \Lambda'}(R)$ from Eq. (8) replacing $A_{\Lambda \rightarrow \Lambda'}^{Eb}(R)$ in Eq. (13).

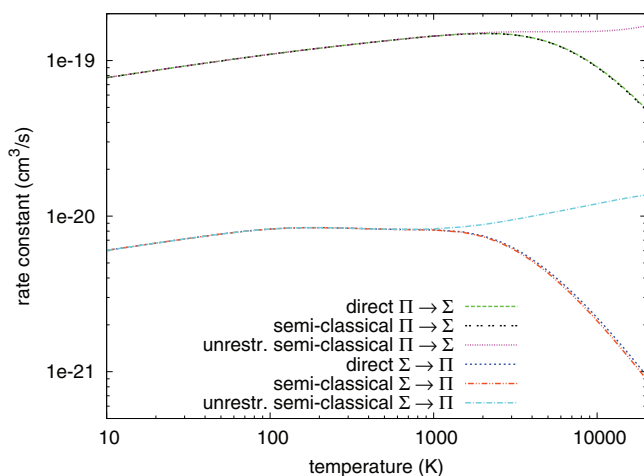


FIG. 4. The rate constant for direct radiative association of SiN through $\Pi \rightarrow \Sigma$ and $\Sigma \rightarrow \Pi$ transitions, computed using cross sections which are obtained in three different ways.

It is clear that the rate constants obtained with semiclassical and perturbation theory combined, which are the best estimates, differ very little from the pure semiclassical rates. At 20 000 K the former exceeds the latter by 1.5% and 5.6% for $\Pi \rightarrow \Sigma$ and $\Sigma \rightarrow \Pi$, respectively. Both of them differ considerably from the unrestricted (conventional) semiclassical result above ~ 2000 K. The direct part of the rate constant can thus be determined with reasonable accuracy with the modified semiclassical formula presented in this work.

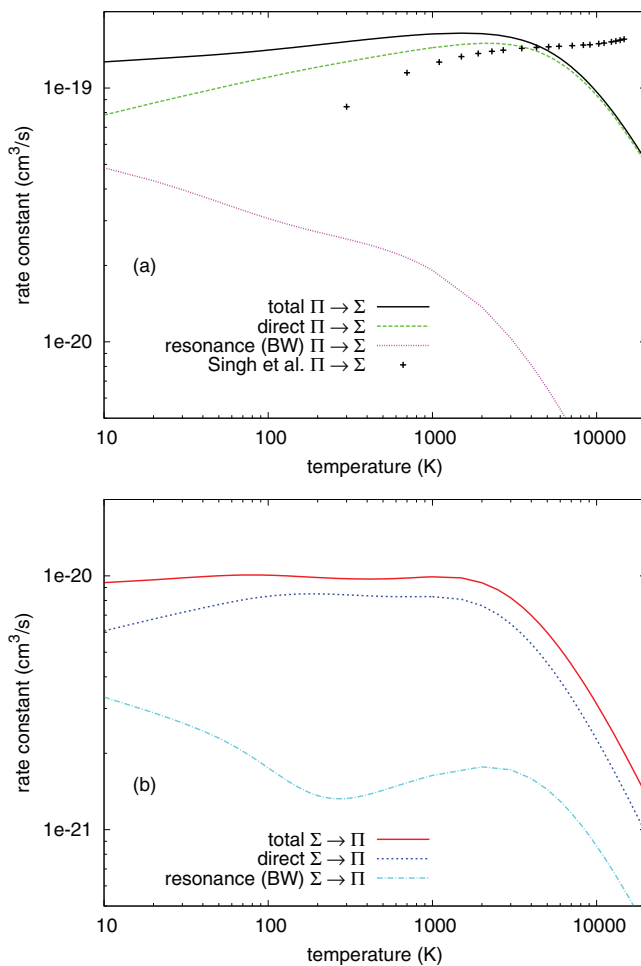


FIG. 5. The rate constant for SiN formation through radiative association through (a) $\Pi \rightarrow \Sigma$ and (b) $\Sigma \rightarrow \Pi$ transitions. Present results are shown with curves and the semiclassical calculation by Singh *et al.*¹⁰ for $\Pi \rightarrow \Sigma$ transitions is shown with symbols.

TABLE IV. Hönl–London factors $\mathcal{S}_{\Lambda S J \Omega \epsilon \Lambda' S' J' \Omega' \epsilon'}$ according to Watson.¹⁷ The approximate values for doublets are obtained by shifting J by one half in two of the factors in the numerator. They are valid for large J .

$2S+1\Lambda$	Ω	ϵ	$2S+1\Lambda'$	Ω'	ϵ'	$J' = J - 1$	$J' = J$	$J' = J + 1$
$^1\Sigma^+$	0	1	$^1\Pi$	0	-1	0	$2J + 1$	0
$^1\Sigma^+$	0	1	$^1\Pi$	0	1	$J - 1$	0	$J + 2$
$^1\Pi$	0	-1	$^1\Sigma^+$	0	1	0	$2J + 1$	0
$^1\Pi$	0	1	$^1\Sigma^+$	0	1	$J + 1$	0	J
$^2\Sigma^+$	1/2	-1	$^2\Pi$	1/2	-1	$\frac{(J-1/2)(J+1/2)}{2J} \approx \frac{J-1}{2}$	0	$\frac{(J+1/2)(J+3/2)}{2(J+1)} \approx \frac{J+2}{2}$
$^2\Sigma^+$	1/2	-1	$^2\Pi$	1/2	1	0	$\frac{(2J+1)(J+1/2)(J+1/2)}{2(J+1)J} \approx \frac{2J+1}{2}$	0
$^2\Sigma^+$	1/2	-1	$^2\Pi$	3/2	-1	$\frac{(J-3/2)(J-1/2)}{2J} \approx \frac{J-1}{2}$	0	$\frac{(J+3/2)(J+5/2)}{2(J+1)} \approx \frac{J+2}{2}$
$^2\Sigma^+$	1/2	-1	$^2\Pi$	3/2	1	0	$\frac{(2J+1)(J-1/2)(J+3/2)}{2(J+1)J} \approx \frac{2J+1}{2}$	0
$^2\Sigma^+$	1/2	1	$^2\Pi$	1/2	-1	0	$\frac{(2J+1)(J+1/2)(J+1/2)}{2(J+1)J} \approx \frac{2J+1}{2}$	0
$^2\Sigma^+$	1/2	1	$^2\Pi$	1/2	1	$\frac{(J-1/2)(J+1/2)}{2J} \approx \frac{J-1}{2}$	0	$\frac{(J+1/2)(J+3/2)}{2(J+1)} \approx \frac{J+2}{2}$
$^2\Sigma^+$	1/2	1	$^2\Pi$	3/2	-1	0	$\frac{(2J+1)(J-1/2)(J+3/2)}{2(J+1)J} \approx \frac{2J+1}{2}$	0
$^2\Sigma^+$	1/2	1	$^2\Pi$	3/2	1	$\frac{(J-3/2)(J-1/2)}{2J} \approx \frac{J-1}{2}$	0	$\frac{(J+3/2)(J+5/2)}{2(J+1)} \approx \frac{J+2}{2}$
$^2\Pi$	1/2	-1	$^2\Sigma^+$	1/2	-1	$\frac{(J-1/2)(J+1/2)}{2J} \approx \frac{J+1}{2}$	0	$\frac{(J+1/2)(J+3/2)}{2(J+1)} \approx \frac{J}{2}$
$^2\Pi$	1/2	-1	$^2\Sigma^+$	1/2	1	0	$\frac{(2J+1)(J+1/2)(J+1/2)}{2(J+1)J} \approx \frac{2J+1}{2}$	0
$^2\Pi$	1/2	1	$^2\Sigma^+$	1/2	-1	0	$\frac{(2J+1)(J+1/2)(J+1/2)}{2(J+1)J} \approx \frac{2J+1}{2}$	0
$^2\Pi$	1/2	1	$^2\Sigma^+$	1/2	1	$\frac{(J-1/2)(J+1/2)}{2J} \approx \frac{J+1}{2}$	0	$\frac{(J+1/2)(J+3/2)}{2(J+1)} \approx \frac{J}{2}$
$^2\Pi$	3/2	-1	$^2\Sigma^+$	1/2	-1	$\frac{(J+1/2)(J+3/2)}{2J} \approx \frac{J+1}{2}$	0	$\frac{(J-1/2)(J+1/2)}{2(J+1)} \approx \frac{J}{2}$
$^2\Pi$	3/2	-1	$^2\Sigma^+$	1/2	1	0	$\frac{(2J+1)(J-1/2)(J+3/2)}{2(J+1)J} \approx \frac{2J+1}{2}$	0
$^2\Pi$	3/2	1	$^2\Sigma^+$	1/2	-1	0	$\frac{(2J+1)(J-1/2)(J+3/2)}{2(J+1)J} \approx \frac{2J+1}{2}$	0
$^2\Pi$	3/2	1	$^2\Sigma^+$	1/2	1	$\frac{(J+1/2)(J+3/2)}{2J} \approx \frac{J+1}{2}$	0	$\frac{(J-1/2)(J+1/2)}{2(J+1)} \approx \frac{J}{2}$

Figure 5 shows the computed total rate coefficients for formation of SiN. Breit–Wigner theory has been used to calculate the resonance contribution according to Eq. (16) and the direct contribution is the same as that in Fig. 4. The rate coefficient for the $\Pi \rightarrow \Sigma$ transition increases steadily up to a maximum of 1.65×10^{-19} cm³/s around 1500 K. The rate for $\Sigma \rightarrow \Pi$ displays slow oscillations and its highest value is 1.01×10^{-20} at about 80 K. Both rates decrease rapidly at temperatures above ~ 2000 K as a consequence of the drop in the cross sections. The semiclassical calculation by Singh *et al.*¹⁰ for $\Pi \rightarrow \Sigma$ is also displayed and it shows no drop at high temperature, as expected since it is based on the unrestricted transition probability. We also see a difference between their result and our direct component (green curve) at low temperatures. This is probably due to a difference in the implementation of the long-range part of the potential.²⁶

The rate coefficients are of interest for modeling of chemistry in the interstellar medium and our results will be made available in the database KIDA.²⁷

V. CONCLUSION

We have calculated radiative association cross sections and thermal rate constants for SiN formation using different approaches. First, we have used perturbation theory. This approach works well, excluding resonances for which the lifetime broadening of the tunneling is smaller than or compar-

able to the lifetime broadening of the radiative decay. This is a natural observation which stems from the perturbation, i.e., the coupling of the molecular system with the electromagnetic field, not being a weak perturbation to the dynamics in these cases. This typically happens for very long-lived quasibound states, which require that the tunneling width and the radiative decay width are both small.

The radiative widths are rather small for all investigated transitions for SiN. It is thus when the tunneling width, which varies by several orders of magnitude, becomes small that we observe long-lived quasibound states and narrow resonances, and this is when perturbation theory is typically observed to break down. As a result, for very narrow resonances, the perturbation theory approach overestimates the peak height and its contribution to the thermal rate constant. This can be overcome by using a quantum dynamical approach with an optical potential that accounts for the decay by spontaneous emission. Even though this method is less demanding than perturbation theory it appears to give the narrow resonances quite accurately. At least the peak heights that we have calculated are in good agreement with those obtained from Breit–Wigner theory which is expected to give all resonances accurately.

At high energies a calculation based on an optical potential with a conventional transition probability has a contribution that does not correspond to molecule formation. This contribution should be excluded in the calculations, which can easily be done by noticing that there exists a corresponding

threshold energy that can be obtained directly from the potentials. Preliminary calculations for $A^{2S+1}\Pi \rightarrow X^{2S+1}\Sigma^+$ radiative association of CO and CN indicate that this threshold behaviour is general. Those cross sections display similar drops at high energies, below which the conventional transition probability gives no discernible transitions to the continuum. In the present form the optical potential method only includes vertical, i.e., Franck–Condon, transitions, but not others. It therefore yields cross sections that drop to zero too quickly as energy is increased towards the threshold. Furthermore, it is very hard to integrate the narrow resonance contributions to the cross sections to obtain thermal rate constants.

For cases where resonances are not important semiclassical theory appears to work well which was seen by comparing to the baselines of the perturbation theory and optical potential approaches. We have found that the semiclassical calculations reproduce the baseline of those cross sections accurately all the way down to as low energies as 0.02 meV, which is as far down as we perform calculations. A restricted transition probability, which accounts for the threshold energy as in the optical potential method, has been applied in our semiclassical treatment. This leads to a drop in the semiclassical cross sections at high energies which improves agreement with the quantum dynamical cross sections.

For thermal rate constant calculations of radiative association we suggest calculating the baseline with the improved semiclassical formula and adding the resonance contribution using Breit–Wigner theory. If the thermal rate constant is desired at high enough temperatures so that kinetic energies above the threshold contributes, the procedure outlined in Sec. IV involving perturbation theory can be used for better accuracy. Unless the temperature is low, a reasonably good estimate for the total rate can be obtained from the new semiclassical expression alone, excluding resonances entirely. For example, the resonance contribution amounts to 17% at 300 K for $\Pi \rightarrow \Sigma$ transitions in SiN, and less at higher temperatures.

ACKNOWLEDGMENTS

This project was supported by the ASTRONET CATS collaboration. Valuable discussions with Gerd Schiffel are gratefully acknowledged. J.F. thanks Daniel Nilsson from the Chalmers C3SE computer center for support.

APPENDIX: HÖNL-LONDON FACTORS

The Hönl–London factors in Table I are defined as

$$S_{\Lambda J \rightarrow \Lambda' J'} = \sum_{\Omega \epsilon'} \mathcal{S}_{\Lambda S J \Omega \epsilon \Lambda' S J' \Omega' \epsilon'}, \quad (\text{A1})$$

where \mathcal{S} are presented in Table IV. The approximate values for doublets in Table IV have been used in this work. The summation over $\Omega \epsilon$ is not done explicitly in the calculations of the cross section in Eq. (4) but it is instead taken care of by multiplication by the factor P_{Λ} .

- ¹J. F. Babb and A. Dalgarno, “Radiative association and inverse predissociation of oxygen atoms,” *Phys. Rev. A* **51**, 3021–3026 (1995).
- ²F. H. Mies, “Resonant scattering theory of association reactions and unimolecular decomposition. I. A united theory of radiative and collisional recombination,” *J. Chem. Phys.* **51**, 787–797 (1969).
- ³J. S. Cohen and J. N. Bardsley, “Calculation of radiative single-charge-transfer cross sections for collisions of He^{2+} with He at low energy,” *Phys. Rev. A* **18**, 1004–1008 (1978).
- ⁴D. R. Bates, “Rate of formation of molecules by radiative association,” *Mon. Not. R. Astron. Soc.* **111**, 303–314 (1951).
- ⁵G. Breit and E. Wigner, “Capture of slow neutrons,” *Phys. Rev.* **49**, 519–531 (1936).
- ⁶R. A. Bain and J. N. Bardsley, “Shape resonances in atom-atom collisions. I. Radiative association,” *J. Phys.* **5**, 277–285 (1972).
- ⁷O. J. Bennett, A. S. Dickinson, T. Leininger, and F. X. Gadea, “Radiative association in $\text{Li} + \text{H}$ revisited: the role of quasi-bound states,” *Mon. Not. R. Astron. Soc.* **341**, 361–368 (2003); **384**, 1743 (2008), erratum.
- ⁸F. Mrugała, V. Špirko, and W. P. Kraemer, “Radiative association of HeH_2^+ ,” *J. Chem. Phys.* **118**, 10547–10560 (2003).
- ⁹S. V. Antipov, M. Gustafsson, and G. Nyman, “Spin-orbit and rotational couplings in radiative association of $\text{C}(\text{}^3P)$ and $\text{N}(\text{}^4S)$ atoms,” *J. Chem. Phys.* **135**, 184302 (2011).
- ¹⁰P. D. Singh, G. C. Sanzovo, A. C. Borin, and F. R. Ornellas, “The radiative association of Si and N atoms, C and O atoms, and C atoms and S^+ ions,” *Mon. Not. R. Astron. Soc.* **303**, 235–238 (1999).
- ¹¹T. H. Dunning, Jr., “Gaussian basis sets for use in correlated molecular calculations. I. The atoms boron through neon and hydrogen,” *J. Chem. Phys.* **90**, 1007–1023 (1989).
- ¹²D. E. Woon and T. H. Dunning, Jr., “Gaussian basis sets for use in correlated molecular calculations. III. The atoms aluminum through argon,” *J. Chem. Phys.* **98**, 1358–1371 (1993).
- ¹³B. E. Turner, “Detection of SiN in IRC + 10216,” *Astrophys. J.* **388**, L35–L38 (1992).
- ¹⁴P. Schilke, S. Leurini, K. M. Menten, and J. Alcolea, “Interstellar SiN,” *Astron. Astrophys.* **412**, L15–L18 (2003).
- ¹⁵P. S. Julienne, M. Krauss, and W. Stevens, “Collision induced $\text{O } ^1D_2 - ^1S_0$ emission near 5577 Å in argon,” *Chem. Phys. Lett.* **38**, 374–381 (1976).
- ¹⁶C. M. Andreazza, P. D. Singh, and G. C. Sanzovo, “The radiative association of C and S, C^+ and S, Si and O, and Si^+ and O,” *Astrophys. J.* **451**, 889 (1995); **475**, 853 (1997), erratum.
- ¹⁷J. K. G. Watson, “Hönl–London factors for multiplet transitions in Hund’s case a or b,” *J. Mol. Spec.* **252**, 5–8 (2008).
- ¹⁸L. D. Landau and L. M. Lifshitz, *Quantum Mechanics Non-Relativistic Theory*, 3rd ed. (Pergamon, Oxford, 1977).
- ¹⁹B. Zygelman and A. Dalgarno, “Radiative quenching of $\text{He}(2^1S)$ induced by collisions with ground-state helium atoms,” *Phys. Rev. A* **38**, 1877–1884 (1988).
- ²⁰P. S. Julienne, “Theory of rare gas–group VI $^1S-^1D$ collision-induced transitions,” *J. Chem. Phys.* **68**, 32–41 (1978).
- ²¹R. J. L. Roy and W.-K. Liu, “Energies and widths of quasibound levels (orbiting resonances) for spherical potentials,” *J. Chem. Phys.* **69**, 3622–3631 (1978).
- ²²R. J. Le Roy, LEVEL 8.0, a computer program for solving the radial Schrödinger equation for bound and quasibound levels, University of Waterloo Chemical Physics Research Report CP-663, 2007.
- ²³D. T. Colbert and W. H. Miller, “A novel discrete variable representation for quantum mechanical reactive scattering via S-matrix Kohn method,” *J. Chem. Phys.* **86**, 1982–1991 (1992).
- ²⁴G. A. Korn and T. M. Korn, *Mathematical Handbook for Scientists and Engineers*, 2nd ed. (McGraw-Hill, New York, 1968).
- ²⁵S. V. Antipov, T. Sjölander, G. Nyman, and M. Gustafsson, “Rate coefficient of CN formation through radiative association: A theoretical study of quantum effects,” *J. Chem. Phys.* **131**, 074302 (2009).
- ²⁶We have used the *ab initio* data of Singh *et al.*¹⁰ without knowledge of how they implemented the short- and the long-range part of the potentials and transition dipole.
- ²⁷V. Wakelam *et al.*, “A kinetic database for astrochemistry (KIDA),” *Astrophys. J., Suppl. Ser.* **199**, 21 (2012).